

## Assessment of method errors in measurement of acceleration fields in accelerating sections of charged-particle accelerators

Aleksandr Evgen'evich Novozhilov, Aleksandr Nikolaevich Filatov, Vladimir Kuz'mich Shilov

National Research Nuclear University "MEPhI", Kashirskoye shosse 31, Moscow, 115409, Russian Federation

**Abstract.** The integral part of the process of creating accelerating sections is the process of their tuning which in its turn should obligatory includes the process of measurement of acceleration field intensity in the transit channel of the accelerating section. This work presents the results of numerical simulation of the processes of measuring acceleration fields in accelerating sections of various radio-frequency charged-particle accelerators operating in the mode of the running and standing wave. Method errors of various types of measurement have been assessed and the comparative analysis of the measurement methods under consideration for the acceleration field in the transit channel of the accelerating section for this type of accelerators has been performed.

[Novozhilov A.E., Filatov A.N., Shilov V.K. **Assessment of method errors in measurement of acceleration fields in accelerating sections of charged-particle accelerators.** *Life Sci J* 2014;11(11s):506-510] (ISSN:1097-8135). <http://www.lifesciencesite.com>. 115

**Keywords:** accelerating system, accelerating section, running wave, standing wave, accelerating resonator, frequency, cell, coupling coefficient, acceleration field intensity, amplitude of acceleration field intensity, acceleration field intensity phase, complex amplitude of acceleration field intensity, small resonant perturbation method, small nonresonant perturbation method

### Introduction

Measurement of fields in high-frequency circuits in general and in accelerating sections of charged-particle accelerators in particular is based on the so called small perturbation methods.

We can distinguish two small perturbation methods, the small nonresonant perturbation method and the small resonant perturbation method, theoretical justification of which is given in works [1, 2]. In particular, in work [2] the following fundamental relationships for nonresonant and resonant perturbation method have been deduced

$$\Delta S_{2,1} = \frac{1}{4\sqrt{P_1 P_2}} \sum_{i=x,y,z} \{j\omega [K_i^{(B)} B_i^{(1)} B_i^{(2)} - K_i^{(E)} E_i^{(1)} E_i^{(2)}] - K_i^{(\sigma)} E_i^{(1)} E_i^{(2)}\}, \quad (1)$$

$$\frac{f_0 - f_0^{(p,b)}}{f_0} = \frac{\sum_i [K_i^{(E)} |E_i|^2 + K_i^{(B)} |B_i|^2]}{4W}. \quad (2)$$

Where  $j$  is the imaginary unit, and coefficients  $K_i^{(E)}$ ,  $K_i^{(B)}$  и  $K_i^{(\sigma)}$  in formulas (1) and (2) are called form factors of the small perturbing body with relevant components ( $i = x, y, z$ ) of the electric field intensity ( $E_i$ ) and magnetic induction intensity ( $B_i$ ) in the point of the small perturbing body.

Form factors of the perturbing body ( $p, h$ ) depend on the form and sizes of the body and the capability of the perturbing body material to magnetize, polarize and carry electrical

current under the influence of the external electromagnetic field.

Formula (1) is the nonresonant perturbation formula and is used, as a rule, for measurement of fields in accelerating sections with the running wave though it can also be used for measurement of fields in accelerating sections with the standing wave. In this formula the value  $\Delta S_{2,1} = \Delta S_{1,2} = S_{2,1}^{(p,b)} - S_{2,1} = S_{1,2}^{(p,b)} - S_{1,2}$  refers to change of the complex coefficient of transfer

from a certain reference plane of the 1st arm to a certain reference plane of the 2nd arm of the multi-armed electrodynamic system under consideration when inserting the perturbing body into it, at that, the electrodynamic system under consideration is considered to be reversible, its scattering matrix is considered to be symmetric, a  $\omega - 2\pi f$  is the angular frequency at which measurements are made.

Where  $S_{2,1} - S_{1,2}$  is the complex coefficient of transfer when the small perturbing body is outside the electrodynamic system under consideration, and  $S_{2,1}^{(p,b)} = S_{1,2}^{(p,b)}$  is the same complex coefficient of transfer when the perturbing body is inserted into the system under consideration. At that,  $P_1$  is the incident wave power in the reference plane of the 1st arm and  $P_2$  is the incident wave power in

the reference plane of the **2nd** arm. In general, the rest of arms, if any, can end up with matched and mismatched loads.

When measuring the fields in the accelerating section, it can be inserted into the measuring circuit either by the four-pole circuit or by the two-pole circuit. In the former case the complex coefficient of transfer  $S_{2,1} = S_{1,2}$  is measured in absence of the perturbing body in the transit channel of the accelerating section and the complex coefficient of transfer  $S_{2,1}^{(p.b.)} = S_{1,2}^{(p.b.)}$  is measured when inserting the perturbing body into the transit channel. In general, complex amplitudes of the electromagnetic field component in the transit channel of the accelerating section in its excitation through the **1st** and through the **2nd** arm differ from each other, that is  $E_i^{(1)} \neq E_i^{(2)}, B_i^{(1)} \neq B_i^{(2)}$  even if  $P_1 = P_2$ .

In the latter case  $P_1 = P_2 = P$ , a  $E_i^{(1)} E_i^{(1)} = (E_i^{(1)})^2$  and  $B_i^{(1)} B_i^{(1)} = (B_i^{(1)})^2$  refer to squares of complex amplitudes of the nonperturbed electromagnetic field component created in the electrodynamic system under consideration in its excitation through the **1st** arm and incident wave power in this arm equal to  $P$ . At that, the rest of the arms (if any) can end up with matched and mismatched loads. In this case  $\Delta S_{1,1} = \Delta \Gamma_1 = \Gamma_1^{(p.b.)} - \Gamma_1$  refers to the change of the complex reflection coefficient in a certain reference plane of the **1st** arm through which the electromagnetic field in the section is excited.

Since in most cases there is only one electromagnetic field component on the axis of the transit channel, namely, the longitudinal component of the electric field intensity, the complex amplitude of which we denote as  $E_z$ , formula (1) will be as follows

$$\Delta \Gamma_1 = \frac{j\omega}{4P} K_z^{(E)} E_z^2. \quad (1.1)$$

Formulas (1) and (1.1) show that the nonresonant perturbation method allows to obtain information both of the absolute value and of the phase of the component of the nonperturbed electromagnetic field of induced oscillations created in the electrodynamic system under consideration in its excitation on the intended frequency  $\omega = 2\pi f$  and under given conditions.

Formula (2) is a resonant perturbation formula and is used to measure the fields in accelerating sections with the standing wave that is in accelerating resonator. In this formula  $\frac{(f_0 - f_0^{(p.b.)})}{f_0}$  refers to the relative shift of the resonant frequency of the resonator mode under consideration when inserting the small perturbing body in its transit channel, and  $f_0^{(p.b.)}, f_0$  refers to the resonant frequency of oscillations of the resonator mode under consideration when inserting the small perturbing body into the resonator and without it.

$E_i, B_i$  refers to complex amplitudes of the component of electric field intensity and intensity of magnetic induction of nonperturbed resonator oscillations at the perturbing body point, and  $W$  refers to the total energy of the electromagnetic field accumulated in the resonator in its excitation on the resonant frequency  $f_0$  of the mode under consideration in absence of the perturbing body.

To measure the longitudinal component of the electric field intensity in the transit channel of the accelerating resonator we can use the following resonant perturbation formula

$$\frac{f_0 - f_0^{(p.b.)}}{f_0} = \frac{\Delta f_0}{f_0} = \frac{K_z^{(E)} |E_z|^2}{4W}. \quad (2.1)$$

### Method

We assume that accelerating sections are chains of interconnected cells. To calculate the complex amplitudes of accelerating voltages on the cells of these sections it is convenient to use their equivalent circuit shown in Fig.1 [3,4,5].

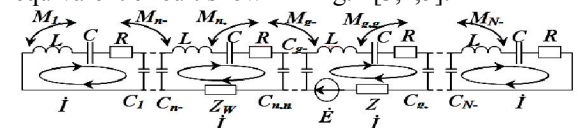


Fig. 1. Equivalent circuit of the accelerating section with the electric and magnetic coupling between cells

Where  $k = 1, 2, 3, \dots, N$  is the cell number and  $N$  is the number of cells in the accelerating section. The cells can be coupled through both the electric field on the section axis (capacity coupling) and the magnetic field, for example, using the peripheral coupling slots (induction coupling). Both of these types of coupling between cells are shown in the diagram as transverse capacitive elements with capacities  $C_{k,k+1}$  and presence of the induction coupling between inductive elements  $L_k$  and  $L_{k+1}$  which is characterized with mutual induction  $M_{k,k+1}$ .

The electromagnetic field in accelerating sections is excited through the cell with the number  $g$  which is reflected in the diagram with presence of the introduced voltage source in the circuit of this cell with the complex amplitude  $\dot{E}_g$  and the introduced wave resistance of the incoming waveguide line  $Z_{Wg}$  through which electromagnetic field in the accelerating section is excited. To simulate insertion of the accelerating section into the measuring circuit by the four-pole circuit presence of the waveguide line is provided which is connected with the  $n$  cell which is reflected in the diagram with presence of the  $n$  cell of the introduced wave resistance of this waveguide line  $Z_{Wn}$  in the circuit. The diagram also reflects contour currents complex amplitudes of which equal to  $I_k$ . Absence and presence of the perturbing body in a certain cell of the accelerating section is simulated so that the frequency of each cell can assume the value  $f_{ck}$  (unperturbed cell frequency) and  $f_{ck}^{(p.b.)}$  (perturbed cell frequency). At that, relative cell detuning induced by the perturbing body is similar for all the cells and is small enough, that is  $(f_{ck} - f_{ck}^{(p.b.)}) / f_{ck} = (\Delta f_c / f_c)_{p.b.} \ll 1$ .

**Main part**

1. Accelerating sections with the running wave.

The electromagnetic field in the accelerating section with the running wave is excited through the incoming waveguide line connected with the first cell [6]. To measure the acceleration field on the axis of the transit channel the section is inserted by the two-pole circuit and the coefficient of reflection in the reference plane of this incoming waveguide line ( $g = 1$ ) is measured.

Figure 2 shows the results of numerical simulation for the accelerating section with the backward running wave with the following parameters:

$$f_{op} = 3 \text{ GHz,}$$

$$\varphi_{op} = 120^\circ, Q_0 = 15000, K_c/2 = 0.01, K_L/2 = -0.02.$$

The upper figure shows the dispersion curve of the infinite uniform structure with the above cell parameters. At that, cell frequencies at which the damping backward running wave is spread in the structure on the operating frequency are equal to  $f_c = 3.014815$  GHz and damping per cell on the operating frequency is equal to  $\exp(-\alpha_{op}D) = 0.9961$ . The cell frequency and operating frequency are marked as points at the dispersion curve. The middle and bottom figures show the results of calculation for distribution of the relative amplitude and the voltage phase on section cells (o) and the results of simulating the changes of these values (x). The number of cells in section  $N = 40$  and perfectly tuned cells should have the following parameters:

$$f_{c1} = 3.007425, f_{c2} = \dots = f_{cN-1} = 3.014815, f_{cN} = 3.007482 \text{ GHz,}$$

$$\chi_1 = 129.438173, \chi_N = 128.438115.$$

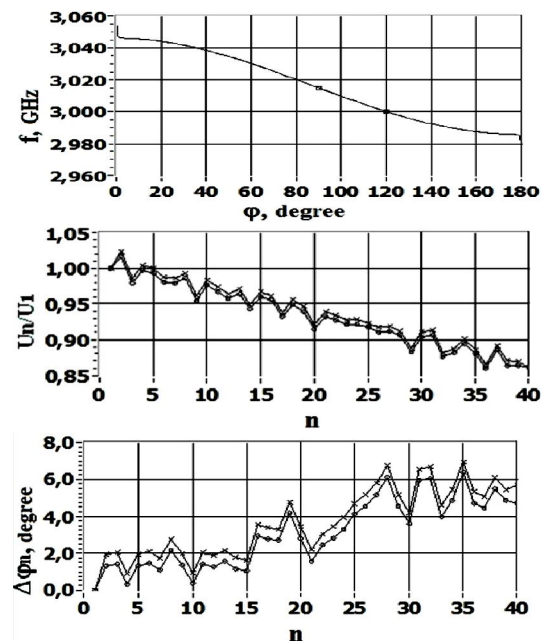


Fig. 2. Distribution of the relative amplitude of voltage and its phase at random cell frequency diversity with uniform distribution within the range  $(\delta f_c / f_c)_{random} = \pm 10^{-4}$ ,  $(\Delta f_c / f_c)_{p.b.} = 10^{-4}$ .

o – no perturbing body; x – measurement numerical simulation.

Complete damping on the operating frequency  $f_{op}$  for the perfectly tuned section is equal to

$$\exp[-(N - 1)\alpha_{op}D] = 0.858679.$$

The above example shows that frequencies of cells have random relative dispersion with uniform distribution within the range  $(\delta f_c / f_c)_{random} = \pm 10^{-4}$  and the relative cell detuning induced by the perturbing body  $(\Delta f_c / f_c)_{p.b.} = 10^{-4}$ .

The analysis showed that maximum distinction between the rated relative voltage amplitude and its phase and the relative voltage amplitude and its phase obtained as a result of simulating their changes is **0.76 – 0.82 %** and **0.96° – 1.00°**, respectively, depending on selection of random scatter of cell frequencies.

In the lower figure the value  $\Delta\varphi_n$  refers to phase differential of voltage on the cell with the number  $n$  and the phase which this voltage should have in perfect tuning of all section cells. Since dispersion of the perfect structure based on which the section under consideration is made, is negative the voltage phase on each cell in the perfectly tuned section is  $\varphi_{ideal n} = +(n - 1)120^\circ$ .

2. Accelerating sections with the standing wave.

We shall confine ourselves to consideration of resonators with the operating  $\pi$  – type oscillations only [7-10]. Due to losses voltage phase differential on adjacent cells will not be exactly **180°**.

The frequency value  $f_{c,g}$  and the coupling coefficient value

**$\chi_g$  should be selected so that** the

reflection coefficient  $\Gamma_{inp}(f_{op})$  on the operating frequency would be minimum (equal to zero). We shall assume that the coupling coefficient  $\chi_n \ll 1$  while the coupling coefficient  $\chi_g$  is rather high. In high quality factor of cells  $\chi_g$  has the value close to the number of cells  $N$ . In reduced quality factor of cells  $\chi_g$  decreases.

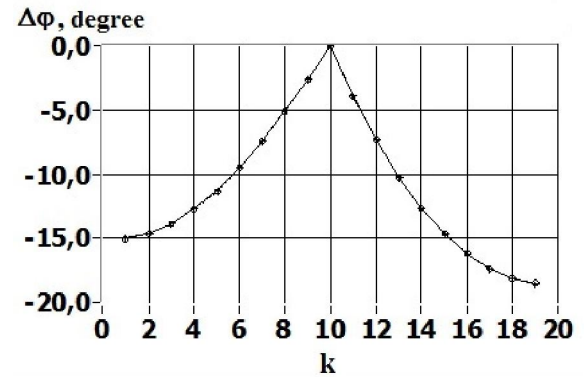
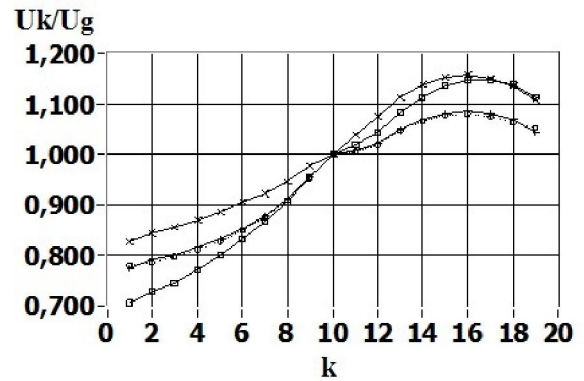


Figure 3 shows an example of such simulation for the resonator with the following parameters:

$$f_{op} = 3,0 \text{ GHz,}$$

$$N = 19, g = 10, n = 1, Q_0 = 15000, K_c/2 = 0.01, \frac{K_i}{2} = -0.02, \chi_n = 10^{-3}.$$

The frequencies of cells in the perfectly tuned resonator should be

$$f_{c1} = f_{c19} = 3.014815, f_{c2} = \dots = f_{c9} = 3.029269, f_{c10} = 3.028909,$$

$$f_{c11} = \dots = f_{c18} = 3.029269 \text{ GHz}$$

and for matching on the operating frequency it is necessary that  $\chi_g = 18.069638$ . In this case

$$\Gamma_{inp}(f_{op}) = 0, \text{ a } |S_{n,g}(f_{op})| = 5.365 \cdot 10^{-5}.$$

In the above example the frequencies of the cells have random relative dispersion with uniform distribution within the range  $(\delta f_c / f_c)_{random} = \pm 5 \cdot 10^{-5}$ , and the relative detuning of the cell frequency induced by the perturbing body is  $(\Delta f_c / f_c)_{p.b.} = 10^{-5}$ . The phase distribution has been obtained using the small nonresonant perturbation method.

As shown from these and other examples the best result can be obtained through the small nonresonant perturbation method which has the smallest systematic error when measuring the

amplitude (in our example **0.2%**) and when measuring the phase the error can be less than **0.5°**.

### Conclusion

The comparative analysis of the methods under consideration to measure the acceleration field in the transit channel of the accelerating section has shown that the small nonresonant perturbation method has the smallest systematic error which can be successfully used in both sections with the running wave and in sections with the standing wave. However, requirements for the perturbing body in the latter case are more rigid. Thus, relative detuning of the cell frequency induced by the perturbing body in this case should not exceed  $(\Delta f_c / f_c)_{p.b.} = 10^{-5}$ . In the first case relative detuning of the cell frequency induced by the perturbing body can be much higher. This is due to the fact that similar relative detuning of the cell frequency results in different perturbation of the field in the resonator and in sections with the running wave in similar parameters of cells (closely spaced frequencies of cells and coupling coefficients between cells).

If the number of the cell through which the resonator is excited and the number of the cell connected with the second arm are not equal ( $g \neq n$ ) it is not reasonable to use the small resonant perturbation method with measurement of the transfer coefficient  $S_{n,g}$  as the measurement error in this case can be unacceptably large. If  $g = n$  both methods for measurement of the resonant frequency of the resonator mode under consideration give approximately the same result.

### Summary

It is not reasonable to use of the small resonant perturbation method in cases when the quality factor of cells and the resonator in general is not high.

### Corresponding Author:

Dr. Novozhilov Aleksandr Evgen'evich  
National Research Nuclear University "MEPhI"  
Kashirskoye shosse 31, Moscow, 115409, Russian Federation

7/9/2014

### References

1. Steele, Charles W., 1966. A Nonresonant Perturbation Theory. IEEE Transactions on MTT, 14(2): 70-74.
2. Nakamura, Masao, 1968. Theory of Field Strength Determination in RF Structures by Perturbation Techniques, Japanese Journal of Applied Physics, 7(2): 146-155.
3. Kaluzhniy, V.E., 2006. Analysis of accelerating structures based on round septate waveguide withequivalent circuit. Engineering Physics, 3: 27-37.
4. Kalyuzhnyi, V.E., A.E. Novozhilov, A.N. Filatov and V.K. Shilov, 2013. Relative Jitter of Accelerating Voltage Amplitude on Resonator's Cells of Linear Electron-positron collider TESLA-ILC. World Applied Sciences Journal, 27(12): 1620-1624. Date Views 10.01.2014 [www.iwdosi.org/wasj/wasj27\(12\)13/14.pdf](http://www.iwdosi.org/wasj/wasj27(12)13/14.pdf).
5. Gavrillov N.M., O.V. Novikov, N.I. Samargin, Yu.N. Strukov and Ye.V. Trihin, 2009. Calculation of geometrical parameters of slowing down systems of type of chains of the connected cavity. Engineering Physics, 2: 14-17.
6. Kalyuzhny, V.E. and O.V. Kalyuzhny, 2008. The analysis of transient and the established mode in much-jacheechnyh accelerating sections with electric and magnetic communication between cells. Engineering Physics, 3: 27-36.
7. Knapp, B.C., E.A. Knapp, G.J. Lucas and J.M. Potter, 1965. Accelerating Structures Resonantly Coupled for High-current Proton Linacs. The First National Particle Accelerator Conference, Washington D.C., NS-12(3): 159.
8. Knapp, B.C., E.A. Knapp, G.J. Lucas and J.M. Potter, 1965. Electrical Behavior of Long Linac Tanks and a New Tank-Coupling Scheme. The First National Particle Accelerator Conference, Washington D.C., Washington D.C., NS-12(3): 623.
9. Zavadtsev A.A., B.V. Zveriev, N.N. Nechaev, N.P. Sobenin and V.V. Stepnov, 1979. The accelerating system of the resonator LEA for 5 MeV energy. Accelerators, 12: 27-32.
10. Zavadtsev A.A., B.V. Zveriev, N.P. Sobenin, 1984. The standing wave accelerating structures. Journal of applied physics, 54(1): 81-87.